Acc. Chem. Res. **2002,** *35,* 385−395

Molecular Dynamics Simulations of Biological Reactions

ARIEH WARSHEL

Department of Chemistry, University of Southern California, University Park Campus, Los Angeles, California 90089-1062

Received July 9, 2001

ABSTRACT

This review considers the author perspective on the emergence of molecular dynamics (MD) simulations of biological processes. It starts with the 1976 simulation of the primary event in rhodopsin, moves to the earliest simulations of enzymatic reactions and electron transfer reactions and ends up with recent simulations of proton translocations and ion transport in proteins. The emphasis is placed on our progress in simulations of actual biological reactions and functional properties, rather than on studies of general properties such as structure and thermal motions. In most cases it has been possible to develop special strategies that capture the relevant dynamics of the given biological process. The predictive power of our early simulations of fast biological process (e.g. vision and photosynthesis) and the insight obtained from these studies is pointed out. Critical examinations of dynamical effects in different biological processes is reviewed. This includes the finding that dynamical effects are unlikely to contribute significantly to enzyme catalysis or to other processes with significant activation barriers. Even in the case of ion channels it is found that the most important effects are associated with energetics rather than dynamics. Nevertheless, MD simulations provide what is probably the most realistic description of the actual reactive events. The resulting insight is crucial in studies of fast photobiological reactions and instructive in cases of slower processes.

I. Introduction

By the early 1970s it became clear that molecular dynamics (MD) simulations could be used in studies of some properties of simple solutions and in exploring the molecular nature of gas-phase reactions of systems with a few atoms. It was much less clear whether MD simulations could contribute to the understanding of biological processes. My feeling was that only very fast biological processes should be explored by MD simulations with the computers of that time. It was clear from my experience with energy minimization[1,2] that MD studies of equilibrium properties of proteins will not converge in a meaningful way. Fortunately, the primary event of the visual process presented an important biological problem that could be explored by direct MD simulations. The 1976 study of this photobiological reaction[3] presented the first MD simulation study of the dynamics of a biological process. Although the subsequent simulation of the short-time dynamics of BPTI[4] pointed toward exciting future directions, it only strengthened my feeling that simulation of long-time dynamical effects would have to wait for much more powerful computers. Furthermore, my experience with modeling enzymatic reactions and discussions with Mike Levitt and Max Perutz strengthened my feeling that the most important biological functions are not controlled by dynamical effects and can be modeled quite effectively by considering the corresponding electrostatic interactions.[2] Nevertheless, the gradual emergence of stronger computers and the interest of me and my co-workers in the details of biological processes resulted in studies of the role of dynamics in most types of biological reactions. This work summarizes our studies of the dynamics of such processes. Related works of other groups are only mentioned briefly and more details are given in ref 5.

II. Dynamics of the Primary Event in the Rhodopsins

The primary event of the visual process starts with the absorption of light by the protonated Schiff base of retinal (PSBR) which is bound to the active site of the protein rhodopsin (see, e.g., ref 6). A related photoisomerization reaction occurs in bacteriorhodopsin (bR). In this case, however, the light energy is used to pump protons across the cell membrane (e.g., ref 6), rather than for the visual excitation.

My initial simulation of the primary event in rhodopsin was performed much before the structure of this protein was available. Thus, I represented the effect of the protein by a simple steric constraint and assumed that the fast dynamics is controlled by a relatively rigid active site. The simulation of the surface crossing dynamics involved a semiclassical trajectory approach, where the molecule started at the Franck−Condon region of the excited state and moved classically until it reached a point with maximum surface-crossing probability, where it jumped to the ground state. The probability for crossing between the surfaces was evaluated quantum mechanically.

My early study[3] and subsequent considerations[7] indicted that the crossing probability for each trajectory is much larger than conventionally assumed in photochemical processes (see discussion in ref 8). Such a crossing "funnel" was previously proposed by Michl[9] for some photochemical processes but has not been reproduced by any time-dependent calculations (we will return to this point below).

Figure 1 shows a typical trajectory starting with the excited 11-cis chromophore. In this and other similar trajectories, the isomerization involved only small overall displacements of the individual atoms because partial

Arieh Warshel received his B.Sc. from the Technion Institute in Israel in 1966. He then earned his M.Sc. in 1967 and Ph.D. in 1969 from the Weizmann Institute. His Ph.D. with Shneior Lifson and collaboration with Mike Levitt are the basis of many current molecular simulation programs. Between 1970 and 1976 he postdocked at Harvard University, returned to the Weizmann Institute, and was an EMBO fellow at the MRC in Cambridge, U.K. In 1976 he joined the Department of Chemistry in the University of Southern California, where he is a professor of Chemistry and Biochemistry. He has pioneered computer-modeling approaches for studies of protein functions. These include the development of consistent treatments of electrostatic energies in proteins, the development of hybrid quantum mechanical/molecular mechanics (QM/MM) approaches for studies of enzymatic reactions, the introduction of molecular dynamics simulations to studies of biological processes, and the introduction of microscopic evaluation of thermodynamics cycles in biological systems. The focus of Warshel's group is on simulations of structure function correlation of biological systems.

10.1021/ar010033z CCC: $22.00
Published on Web 04/04/2002

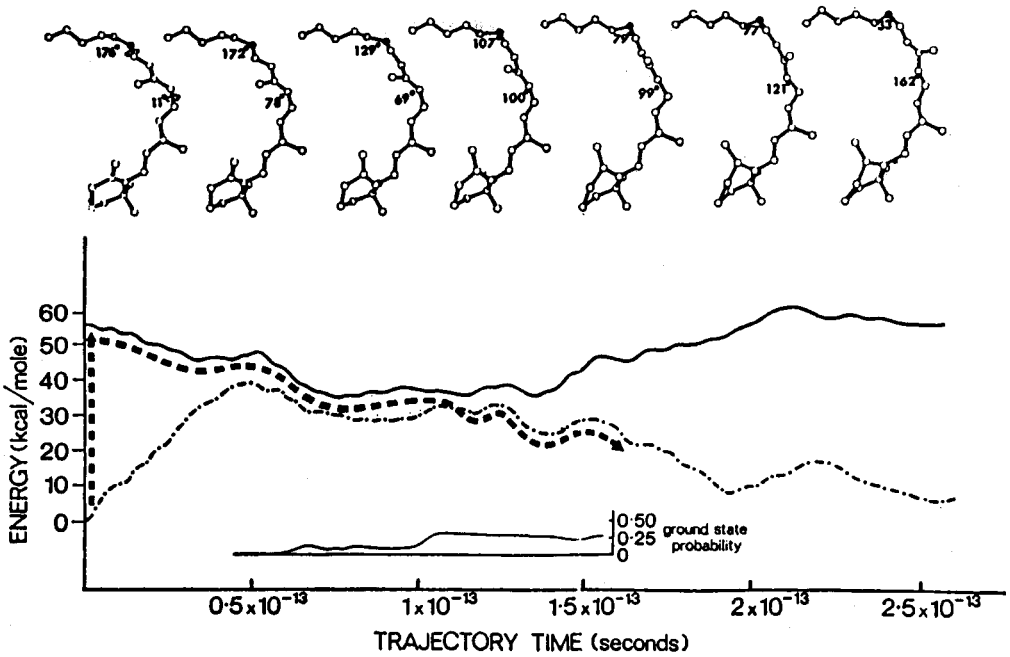

FIGURE 1. Semiclassical simulation of the photoisomerization reaction of rhodopsin. The upper and middle panels describe, respectively, the geometries and energies along a trajectory that moves from the cis configuration to the crossing point ($\phi \approx 90°$) and then crosses to the ground state. The lower panel depicts the probability of being in the ground state. Reprinted with permission from ref. 3. Copyright 1976 *Nature*.

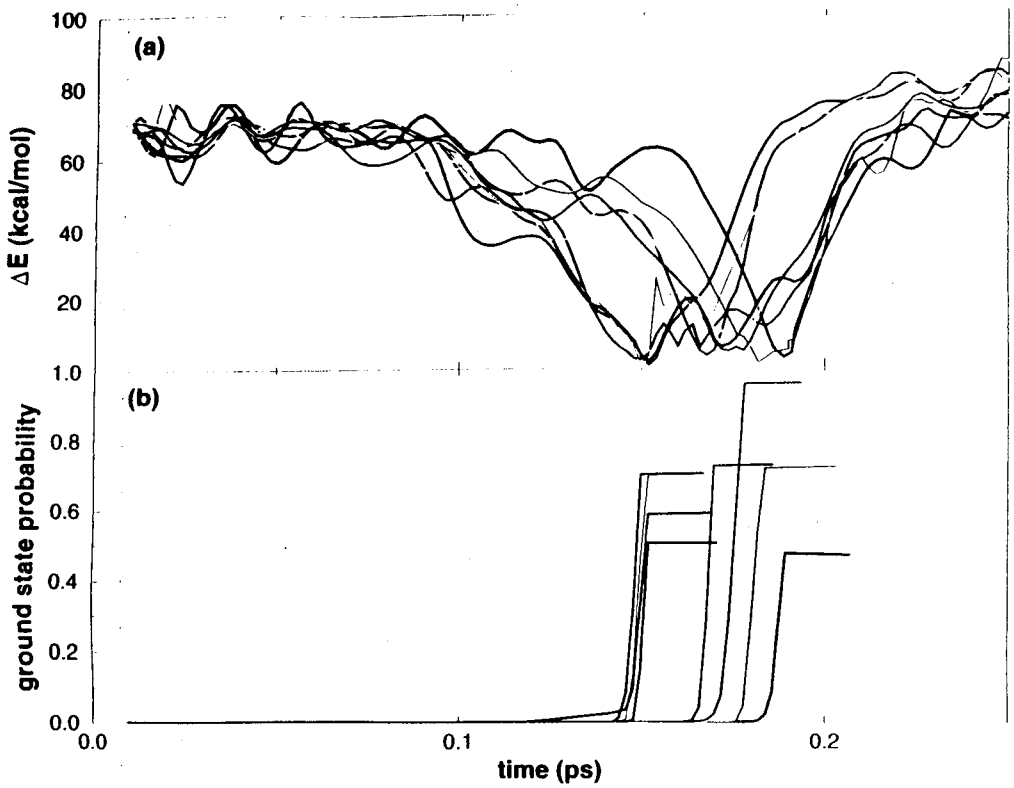

FIGURE 2. (a) Time-dependent energy gaps between the ground and excited states of bacteriorhodopsin during 10 trajectories propagated on the excited state. (b) Probability of being in the ground state during the trajectories shown in a. Reprinted with permission from ref 8. Copyright 2001 American Chemical Society.

rotations occur around several bonds in addition to the $C_{11}-C_{12}$ bond (see ref 10 for discussion). The simulations suggested that the time constant for isomerization was about 100 fs. The predicted time constant was considerably shorter than the time constant of 6 ps that had been obtained in pioneering experimental work by Rentzepis and co-workers,[11] but proved to be in good agreement with subsequent measurements (e.g., ref 12).

The emergence of the three-dimensional structure of bR[13] made it possible to reexamine our early simulation

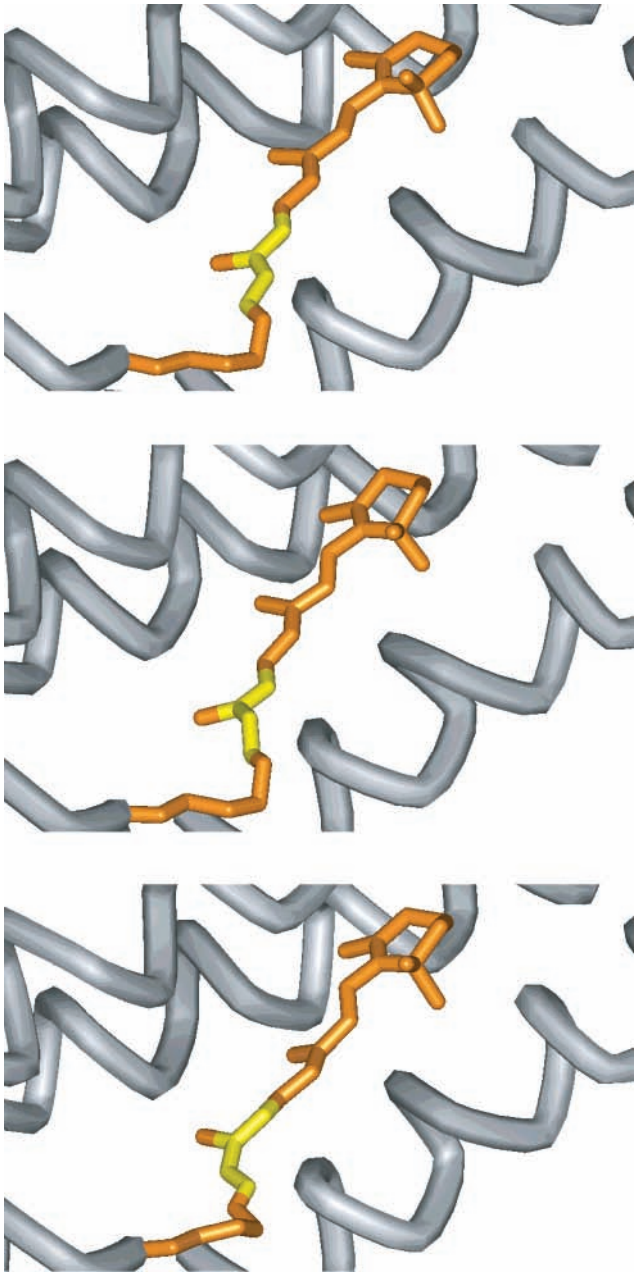

FIGURE 3. Snapshots from a surface crossing trajectory of bR. Reprinted with permission from ref 8. Copyright 2001 American Chemical Society.

with a more realistic protein active site. In a 1991 study,[14] we examined the nature of the excited-state dynamics and found it to correspond to diffusive rather than inertial motion.[14] This finding helped us to exclude several mechanistic options, taking into account the detailed structures of the proteins.

In recent work,[8] we have recalibrated the QCFF/PI surfaces of the PSBR and used a hybrid QM/MM approach to explore the quantum dynamics of the primary event in bR. Ten semiclassical trajectories were run, starting with different initial conditions. Figure 2a shows the calculated energy gaps (ΔE) during the trajectories, and Figure 2b shows the probabilities of finding the system in the ground state. Typical structures of the system along a surface-crossing trajectory are shown in Figure 3.

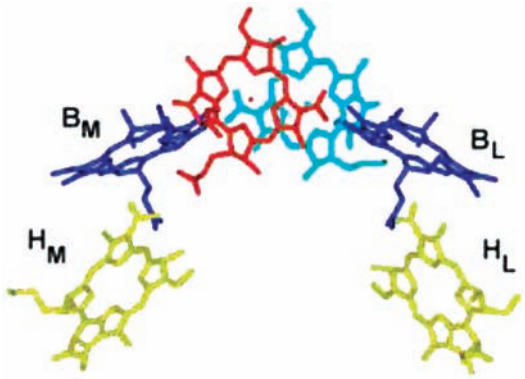

FIGURE 4. Chromophores in the L and M branches of bacterial RCs.

As can be seen in Figure 2a, some of the bR trajectories reach a minimum value of ΔE (ΔE_{min}) of around 1 kcal/mol, while others have larger values of ΔE_{min}. Evidently, crossing can occur either with an actual conical intersection or at points with a larger ΔE where the electronic coupling is sufficiently strong.[8] Although we now have a clearer picture of the structure of rhodopsin, the original prediction[3] (of a very fast process with a very large crossing probability at the 90° region) apparently remains valid.

Related simulation studies are considered in ref 5. They include the one-dimensional studies of Birge and co-workers (e.g., ref 6) and the extensive studies of Schulten and co-workers (e.g., ref 15). The later surface crossing studies included the entire protein−chromophore system but have not yet involved a fully coupled QM/MM treatment (see discussion in ref 8)

III. Dynamics of Photosynthesis and Other Biological ET Reactions

The realization of the power of the semiclassical trajectory approach in treatments of complex systems led me in 1982 to the development of the first microscopic simulations of electron-transfer (ET) reactions in condensed phases.[16] My co-workers and I also introduced studies of quantum mechanical nuclear effects in biological systems, by exploring the electron-transfer rate in cytochrome *c*.[17] The methods mentioned above were used by Bill Parson, our co-workers, and me in the first realistic simulation of the primary ET in bacterial photosynthesis.[18] These and related studies will be reviewed below.

The initial photochemical electron-transfer reactions in photosynthetic bacteria is carried out by pigment−protein complexes called reaction centers (RCs; see, e.g., ref 19 for a review). Reaction centers of purple bacteria typically contain four molecules of bacteriochlorophyll (BChl), two molecules of bacteriopheophytin (BPh), two quinones, and an iron atom. The structures of RCs from two species of bacteria have been solved by X-ray crystallography (see ref 20 and also references in ref 19). In both species, the pigments are bound to two polypeptides, "L" and "M" (see Figure 4). Two of the BChls sit close together, forming what is termed the "special pair" (P). The other BChls (B_L and B_M) and the BPhs (H_L and H_M) sit in the L and M branches.

When RCs are excited with light, the excitation energy moves to P within about 100 fs and the excited dimer (P*) transfers an electron to one of the BPhs (H_L) with a time constant of about 3 ps (e.g., ref 21).

There are two main mechanistic options for the primary event involved: (i) a stepwise process in which the electron jumps from P* to B_L and forms a $P^+B_L^-$ radical pair, which then passes an electron to H_L and forms $P^+H_L^-$, and (ii) a direct jump of the electron from P* to H_L, with $P^+B_L^-$ serving to increase the coupling between the initial and final states through a superexchange mechanism.

Initial unsuccessful attempts to detect $P^+B_L^-$ after excitation of RCs with subpicosecond flashes led to an almost consensus view (see references in ref 19) that the primary charge separation process involves a superexchange mechanism. However, we felt that the experimental information was inconclusive and that the most crucial missing information was the energetics of $P^+B_L^-$. Thus, in 1987, when we finally obtained the crystal structure of *Rhodobacter sphaeroides* (*Rb. Sphaeroides*),[22] we combined all the methods developed in our studies of ET reactions and simulated the dynamics of the charge separation in bacterial RCs. The transitions from P* to $P^+B_L^-$ and from $P^+B_L^-$ to $P^+H_L^-$ were simulated by the surface crossing approach[16] and were incorporated into the coupled differential equations for the concentrations of P*, $P^+B_L^-$, and $P^+H_L^-$.[18] The results agreed qualitatively with the experimental observations. Figure 5 shows a similar simulation using the *Rhodopseudomonas viridis* (*Rp. viridis*) structure. The simulation suggested that the superexchange makes relatively little contribution to the overall rate of charge separation. Most importantly, the energetics of $P^+B_L^-$ was found to be in a range that allows a stepwise mechanism to operate (in a clear contrast to the prevailing view at that time).

Our finding that the two-step mechanism is a very realistic possibility was based on careful application of free energy perturbation (FEP) and other strategies for evaluation of electrostatic energies in proteins. Our calculations (e.g., refs 18 and 23), placed this state 2−3 kcal/mol below P* with an estimated uncertainty of ±3 kcal/mol. Experimental estimates of the free energy of $P^+B_L^-$ were obtained subsequently (see ref 5) and were found to be about 1 kcal/mol below P*, in reasonably good agreement with the computational results.

There is now a general agreement that the P* → $P^+B_L^-$ → $P^+H_L^-$ is the dominant pathway of charge separation at room temperature (e.g., refs 5 and 24). It is gratifying that our simulations predicted the corresponding energetics and elucidated the actual mechanism.

Further MD simulations of electron transfer in photosynthetic reaction centers have been described by several groups of investigators (see the review in ref 5). The early series of these studies[25,26] supported the superexcange mechanism due to incomplete treatment of the electrostatic energy of the system (see ref 5).

Our simulation studies also provided the first molecular insight into quantum mechanical nuclear tunneling in biological systems. During the early 1980s we realized that we could convert our time-dependent energy gap to the Franck−Condon factors and vibrational frequencies of the system and ultimately to the relevant quantum nuclear rate constant. The resulting dispersed polaron approach

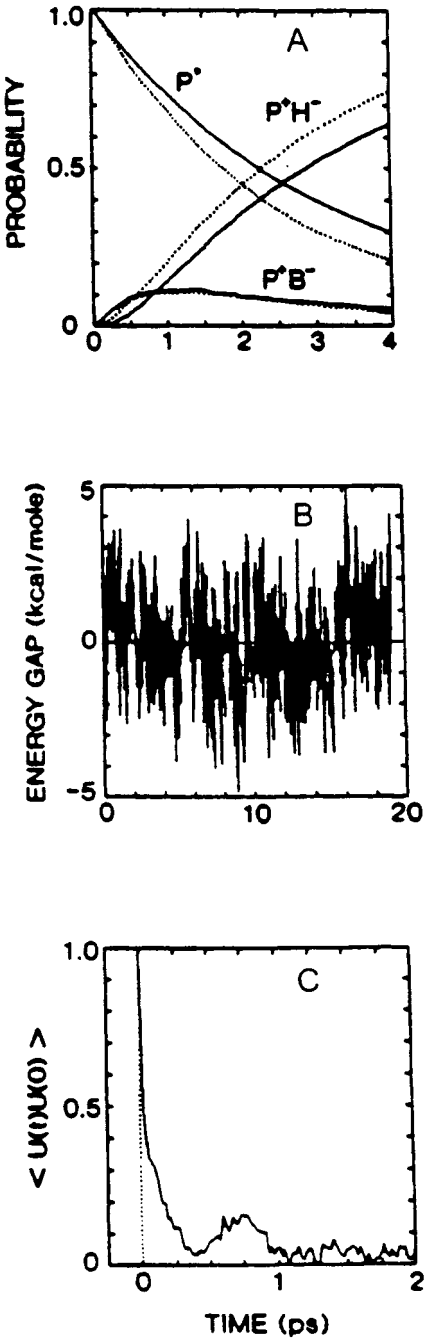

FIGURE 5. Simulations of electron transfer from P* to H_L via B_L in the *Rb. sphaeroides* reaction center. The simulations in panel A used the semiclassical surface-hopping formalism and were based on the time-dependent energy gap between P* and $P^+B_L^-$ ($\Delta\epsilon_{12}$) during in a 20-ps trajectory in P* and of the gap between $P^+B_L^-$ and $P^+H_L^-$ ($\Delta\epsilon_{12}$) during a similar trajectory in $P^+B_L^-$. The simulations shown with *dotted curves* included superexchange; those shown with *solid curves* did not. The energy gap for the P* → P^+B^- process and the corresponding autocorrelation are given in panels B and C, respectively. Reprinted with permission from ref 5. Copyright 2001 Cambridge University Press.

(e.g., refs 17, 27, and 28) rests formally on an exact quantum mechanical expression for electron transfer in a multidimensional harmonic system.[29] However, an evaluation of this expression requires knowledge of the vibrational frequencies (the ω's) and the dimensionless displacements (the d's) between the product and reactant states, for all the modes of the system. While the formal rate expression is well-known, the trick is to obtain the d's and the ω's for the enormous protein/solvent system. Here we realized that the Fourier transform of the energy gap contains all the relevant information. The formulation leads to the relationship

$$\lambda = \frac{1}{2}\sum_j \hbar\omega_j d_j^2 = \frac{1}{2\pi k_B T}\left|\int_{-\infty}^{\infty} J(\omega)\, d\omega\right| \qquad (1)$$

where λ is the overall reorganization energy, which can be obtained from $\Delta\epsilon_{12}(t)$,[19] and k_B is the Boltzman constant. The function $J(\omega)\tanh(\hbar\omega/2k_BT)/2\hbar$ is the so-called "spectral density function". The main point is the realization that the vibrational frequencies and displacements obtained by analyzing an MD trajectory at a single high temperature gives the information needed to describe the complete temperature dependence of the kinetics.

IV. Enzyme Dynamics Not an Important Biological Role

The idea that "dynamical" effects contribute significantly to enzyme catalysis has frequently been invoked (see references in ref 30). The appeal of this idea may reflect the fact that enzymatic reactions involve thermal fluctuations. However, all chemical reactions involve random thermal motions, and it is unlikely that enzymes use particular vibrational modes to enhance reaction rates. To address this issue, we will define the rate constant and clarify what is meant by dynamical effects.

It is now generally agreed that the rate constant for chemical reactions in condensed phase can be written as (see references in ref 30):

$$k = \kappa k_{TST} \qquad (2)$$

where k_{TST} is the transition-state theory rate constant and κ is the "transmission factor", which accounts for the correction of the non-recrossing. In a multidimensional system, the TST rate constant can be expressed as (e.g., ref 31)

$$k_{TST} = \frac{1}{2}\langle|\dot{x}|\rangle_{TS} \exp\{-\Delta g^{\ddagger}/k_BT\}/\int_{-\infty}^{x^{\ddagger}} \exp\{-\Delta g/k_BT\}\, dx \qquad (3)$$

where $\Delta g(x)$ is the free energy functional that describes the probability of being at different points along the reaction coordinate,[31] x; $x^{\ddagger}$ is the value of x at the transition state; $\dot{x}$ is the velocity and $\langle\ \rangle_{TS}$ designates an average over TS configurations. Here, $\Delta g^{\ddagger}$ is the difference between $\Delta g(x)$ at the TS and the minimum of Δg.

The transmission factor can be determined by running trajectories at the TS region and monitoring their downhill time evolution. The time reversal of such trajectories (e.g., ref 32) produces the rare reactive trajectories and can be used to evaluate κ. This is usually done by a counting approach (e.g., ref 32; see also ref 5). However, we will use an alternative approach below.

The factor $\exp\{-\Delta g^{\ddagger}/k_BT\}$ in the TST expression for the rate constant is simply a probability factor that could be evaluated by a nondynamical approach such as Monte Carlo (MC) simulations. Thus, if we can estimate the rate constant correctly by MC approaches, there are no dynamical effects. Furthermore, it is generally accepted that any dynamical effects on the rate must lie in the transmission coefficient κ. The main question, therefore, is whether κ is much greater in some enzymatic reactions than in the corresponding reactions in solution. We will address this question below.

To simulate enzymatic reactions, we developed hybrid quantum mechanical molecular mechanics (QM/MM) approaches[2,30] and in particular developed and advanced the empirical valence bond (EVB) approach.[31]

The EVB approach has been used extensively in studies of the energetics and dynamics of enzymatic reactions, including the first simulations of the dynamics of chemical reactions in enzymes[33] and solutions.[16] Here, we use this method to examine the dynamics of the hydride transfer reaction of alcohol dehydrogenase (ADH).

This reaction is described by the two valence-bond-like (VB-like) resonance structures shown in Figure 6. The potential surfaces of the VB structures are described by analytical potential functions that include the interactions of the charges in each VB structure with their environment. That is, the energies of the VB states are expressed as

$$\epsilon_i = \alpha_{gas}^{(i)} + U_{intra}^{i}(R,Q) + U_{Ss}^{i}(R,Q,r,q) + U_{ss}(r,q) \qquad (4)$$

Here, R and Q represent the atomic coordinates and charges of the VB structures, and r and q are those of the surrounding protein and solvent. $\alpha_{gas}^{(i)}$ is the gas-phase energy of the ith VB structure at infinite separation between the fragments; $U_{intra}^{i}(R,Q)$ is the intramolecular potential of the solute system; $U_{Ss}^{i}(R,Q,r,q)$ represents the interaction of the solute atoms (S) with the surrounding solvent and protein atoms (s); and $U_{ss}(r,q)$ represents the potential energy of the protein/solvent system ("ss" designates surrounding−surrounding). The mixing of the resonance structures gives the ground-state potential surface for the reaction in its particular environment.[31]

To illustrate the factors that control the reaction, we present in Figure 7 a typical reactive trajectory. As seen from the figure, the barrier for hydride transfer oscillates with the fluctuations of the environment surrounding the bound substrate. Once in a while the environment reaches a configuration where the barrier is small and the hydride can be transferred. Thus, the rate of hydride transfer depends on the fluctuations of the surrounding active site and the resulting fluctuations of the potential of the two VB states energies ϵ_1 and ϵ_2. A closer look at the connection between the fluctuations of the environment and the

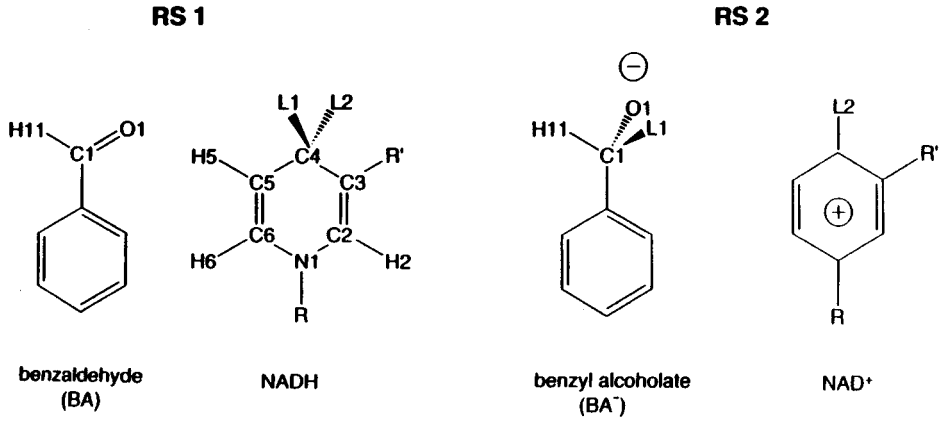

FIGURE 6. Resonance structures used in the EVB description of ADH.

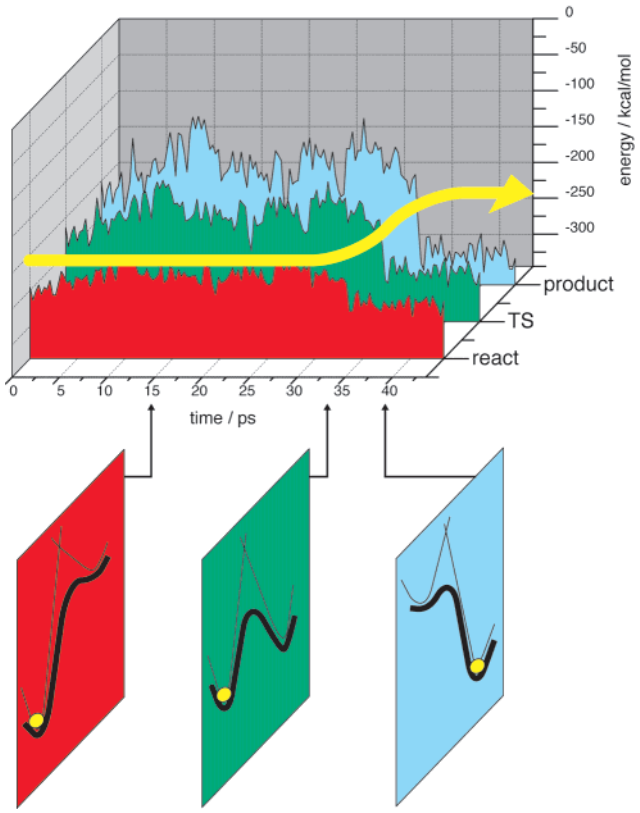

FIGURE 7. Illustrating the effects of the fluctuations of ϵ_2 and ϵ_1 on the reaction of ADH. The figure depicts the time dependence of the ground-state energy profile E_g. This energy is plotted at reactants, transition state, and products. The data have been obtained along an artificially generated (by artificially changing $\alpha_{gas}^{(2)}$ (see ref 30)) reactive trajectory that involves hydride transfer from the NADH to the benzyl aldehyde substrate. The chance for the reaction depends on the average of the fluctuating activation barrier $\Delta E^{\ddagger}$. The lower panels show the ground-state potential at different points along the trajectory.

chance of a charge-transfer reaction illustrates (e.g., refs 16, 30, and 33) that the rate constant reflects the fluctuations of the energy gap $\Delta\epsilon = \epsilon_2 - \epsilon_1$ and in particular the electrostatic contributions to the energy gap. However, the chance for having the proper electrostatic fluctuations probably is determined by the corresponding Boltzman probability.

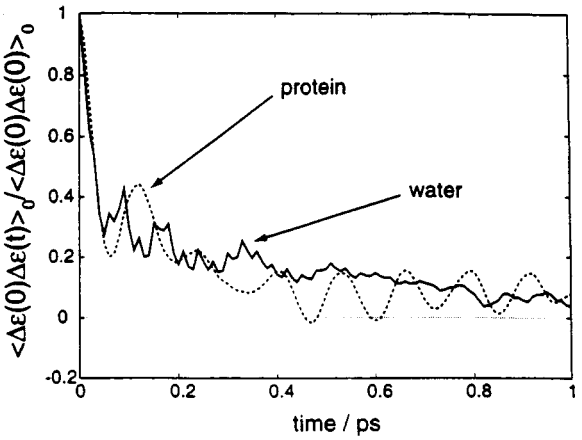

FIGURE 8. Autocorrelation of the electrostatic contributions to the energy gap in ADH and in solution. The oscillations in the protein autocorrelation function are due primarily to movements of the Zn^{2+} ion. Reprinted with permission from ref 30. Copyright 2001 American Chemical Society.

EVB calculations of diverse types of enzymatic reactions (see the review in refs 31 and 30) reproduced repeatedly the reduction of the activation barrier, $\Delta\Delta g^{\ddagger}$, when moving from water to the protein active site. The largest contribution to this $\Delta\Delta g^{\ddagger}$ was found to be due to electrostatic effects of the protein. This electrostatic effect appeared to be associated with the fact that the enzyme dipoles are preorganized toward the TS charges and thus the reorganization energy is reduced significantly.[31,34]

The finding that the largest catalytic contribution comes from the electrostatic part of $\Delta g^{\ddagger}$ cannot be used by itself to exclude the possibility that other contributions also are significant. Here we review the use of our simulation approaches in studies of dynamical contributions to catalysis.

Using the linear response approximation, we were able to show (e.g., ref 31) that the transmission factor is determined by the autocorrelation of the energy gap $\Delta\epsilon(t)$. Thus, we could compare the transmission factors (and the corresponding dynamical effects) of reactions in protein and solutions by comparing the autocorrelation functions of $\Delta\epsilon(t)$. Such a comparison is shown in Figure 8, and a similar comparison was done in our early studies (e.g.,

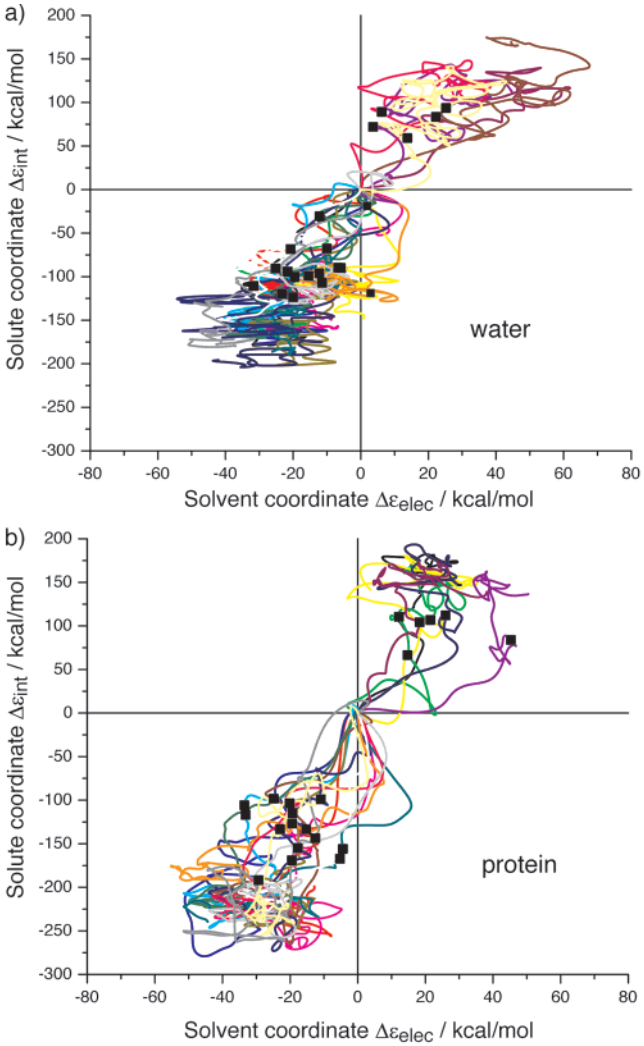

FIGURE 9. Downhill classical trajectories on the ground-state EVB surface (a) for the hydride transfer reaction catalyzed by ADH and (b) for the corresponding reaction in solution. The time reversals of the downhill trajectories correspond to the actual reactive trajectories. The figure represents the reactive trajectories in terms of the solute and solvent coordinates (see ref 30 for more details).

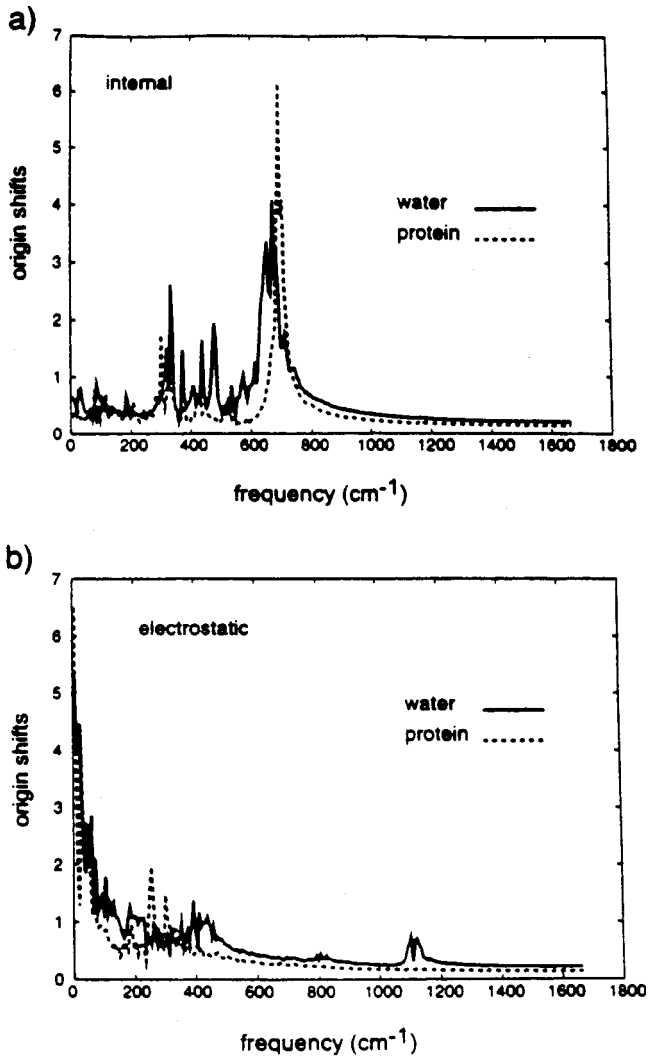

FIGURE 10. $J(\omega)$ in ADH and in solution: (a) contribution of the internal modes of to the reacting system; (b) contribution of the "generalized" solvent coordinate. Reprinted with permission from ref 30. Copyright 2001 American Chemical Society.

ref 31). In all cases it appears that the two autocorrelation functions are similar.

Since the dynamical effects are similar in proteins and solutions, they are unlikely to contribute to catalysis. Interestingly, a direct evaluation of κ in a proton-transfer reaction in triosephosphate isomerase (TIM)[35] found that κ is close to unity. This shows that there is no significant dynamical effect in the enzymatic reaction.

The fact that the dynamical nature of chemical reactions in enzymes and solutions are similar is also illustrated in Figure 9. The figure examines the nature of the reactive trajectories and demonstrates that the reactive trajectories have a similar nature in ADH and in solution.

It is frequently proposed that enzymes use coherent motions or undissipated thermal energy in catalyzing their reactions (see discussions in refs 5 and 30). To examine this proposal, we used our dispersed polaron approach (see section III). This approach was applied to several enzymes (e.g., ref 36), and the results of a recent study of the reaction of ADH[30] is depicted in Figure 10. The figure presents the $J(\omega)$of eq 1 for the reaction in the enzyme and solution, and this compares the biologically relevant vibrations in both cases. As seen from the figure, the $J(\omega)$'s are similar in the enzyme and solution reactions. Thus, it is not likely that the protein accelerates its reaction by increasing specific $J(\omega)$'s. In fact, even in cases where the $J(\omega)$'s are different, we would not necessarily have coherent dynamical effects. For example, if specific coherent modes were acting in ADH, we would not have the results presented in Figure 9, where the reactive trajectories appear to involve random motions.

Our simulation approaches also allowed us to explore the nature of so-called "nonequilibrium solvation" (NES) effects (for a definition of this term, see ref 30). We focused on proposals that these effects are fundamentally different in enzymes and in solution[35] and that this leads to dynamical contributions to catalysis.[37] It was found that NES effects contribute mainly to $\Delta g^{\ddagger}$, rather than to κ.[30] It was also found[30] that alternative approaches for calcula-

tions of NES effects are problematic. Our studies have shown that NES effects reflect mainly the difference in reorganization energies (and the corresponding $\Delta g^{\ddagger}$) between the enzyme and solution reactions. These are probabilistic rather than dynamical effects.

Finally, we were able quite early[36] to examine proposals that quantum mechanical nuclear tunneling effects contribute to enzyme catalysis. For this purpose, we adopted the centroid path integral idea[38,39] but had to introduce important modifications to make this approach effective in studies of chemical reactions in solution and enzymes. The resulting quantized classical path (QCP) approach (see ref 36 and references in ref 30) evaluates quantum mechanical free energies by constraining the center of the quasiparticles to move on the classical potential. The QCP approach provided the first simulations of quantum mechanical nuclear effects in enzymes and solutions (e.g., ref 36). The simulations demonstrated that the quantum effects are significant but are *unlikely* to contribute to catalysis. That is, we found that the quantum mechanical corrections are similar in enzyme and solution and thus do not change $\Delta\Delta g^{\ddagger}$.

V. Proton Translocations and Ion Transport

Proton translocations and ion transport play a major role in biological systems. Our studies of such systems[34,40,41] have focused on the reduction of the barrier for ion transport through low dielectric membranes by the polar groups of the channel. However, the examination of the corresponding time evolutions are also instructive. Two examples are given below.

(a) Proton Translocation Pathways. To explore the nature of biological proton translocations, we studied the proton-transfer pathways in the quinone site of *Rd. sphaeroides*.[42] These processes occur on a microsecond time scale and involve a rather complex control by the protein environment. The protons can jump between internal water molecules and/or protein ionizable residues. The energetics of these jumps are controlled by the surrounding protein. To capture the physics of such a processes, we designed a special "trick" that provides the relevant energetics on-the-fly during calculations of the time evolution of the system. Our starting point is the evaluation of the free energy of the proton at any possible protonation site (including water molecules in the protein cavities and ionizable protein residues). This was done in a semimacroscopic way using[34,40,43]

$$\Delta G^{(m)} = \sum_i (-2.3RTq_i^{(m)}[\mathrm{p}K_{\mathrm{int},i}^{\mathrm{p}} - \mathrm{pH}] + (1/2)\sum_{i\neq j} W_{ij}q_i^{(m)}q_j^{(m)}) \quad (5)$$

where m designates the vector of the charge states in a given configuration. Here $q_i^{(m)}$ is the charge of the ith group at the mth configuration. The $W_{ij}q_i^{(m)}q_j^{(m)}$ term represents the charge−charge interactions. The intrinsic pK_a (pK_{int}) is the pK_a that the given ionizable group would have if all other ionizable groups were kept in their neutral states. The first term in eq 5 is evaluated by our semimacroscopic approach (e.g., ref 40). However, the most important approximation in eq 5 is the use of an effective dielectric constant for charge−charge interaction. That is, we used

$$W_{ij} = 332/(r_{ij}\epsilon_{ij}) \quad (6)$$

where W is given in kilocalories per mole and r in angstroms and ϵ_{ij} is a distance-dependent dielectric constant.[40] The calculated $\Delta G^{(m)}$ terms are then converted to activation barriers using the modified Marcus equation[31] and then used to evaluate the rate constants for all the individual steps.

Since our approach provides the energetics for any possible charge state of the system, we can use it on-the-fly to solve the time evolution of the proton translocation process. This can be done by Brownian dynamics (BD), but in the case of RC we used a master equation for the relevant kinetics. The simulation indicated that the overall time dependence is largely controlled by the energetics of the different protonation sites and not by dynamical effects (see the discussion in ref 40).

(b) Ion Channels. The elucidation of the structure of a bacterial potassium channel (KscA from *Strepomyces lividans*)[44] presents the challenge of simulating current−voltage relationships of an actual biological ion channel. The first step in this direction involved calculations of the ion permeation energy (e.g., refs 45 and 46 and references therein). Unfortunately, with the exception of the work of Aqvist and Luzhkov,[45] most microscopic studies produced unrealistic energetics with enormous barriers. This reflects probably the use of improper boundary conditions and improper treatments of long-range electrostatic interactions.

Moving to the next step of simulating the ion current presents an enormous challenge. It is obvious, for example, that brute force microscopic simulations will be impractical until we have much more powerful computers. On the other hand, phenomological models can provide a useful general insight, but cannot capture the detailed physics of the specific channel (see ref 47).

We have exploited the trick used in the proton translocation study[40,43] and expressed the energy of the system as

$$\Delta G = \sum_k \Delta G_{\mathrm{self}}(r_i) + \sum_{ij}{}' \Delta G_{ij} + \sum_{ik} \Delta G_{ik} + \sum_{ip} (\Delta G_{\mathrm{vdw}})_{ip} \quad (7)$$

where ΔG_{self} is the semimacroscopic estimate of the free energy of a single ion in the protein (with all ionizable groups in their uncharged form); i and j run on the ions, k on the protein ionizable groups, and p over the protein groups in the channel interior. ΔG_{self} is estimated by our PDLD/S-LRA approach,[40] while ΔG_{ij} and ΔG_{ik} are obtained by the analytical expression of eq 6. ΔG_{vdw} is the van der Waals interaction between the ions and the channel interior, which is evaluated by using a simple grid representation for the channel surface. Combining the free energy surface of eq 6 with BD simulations enabled us to

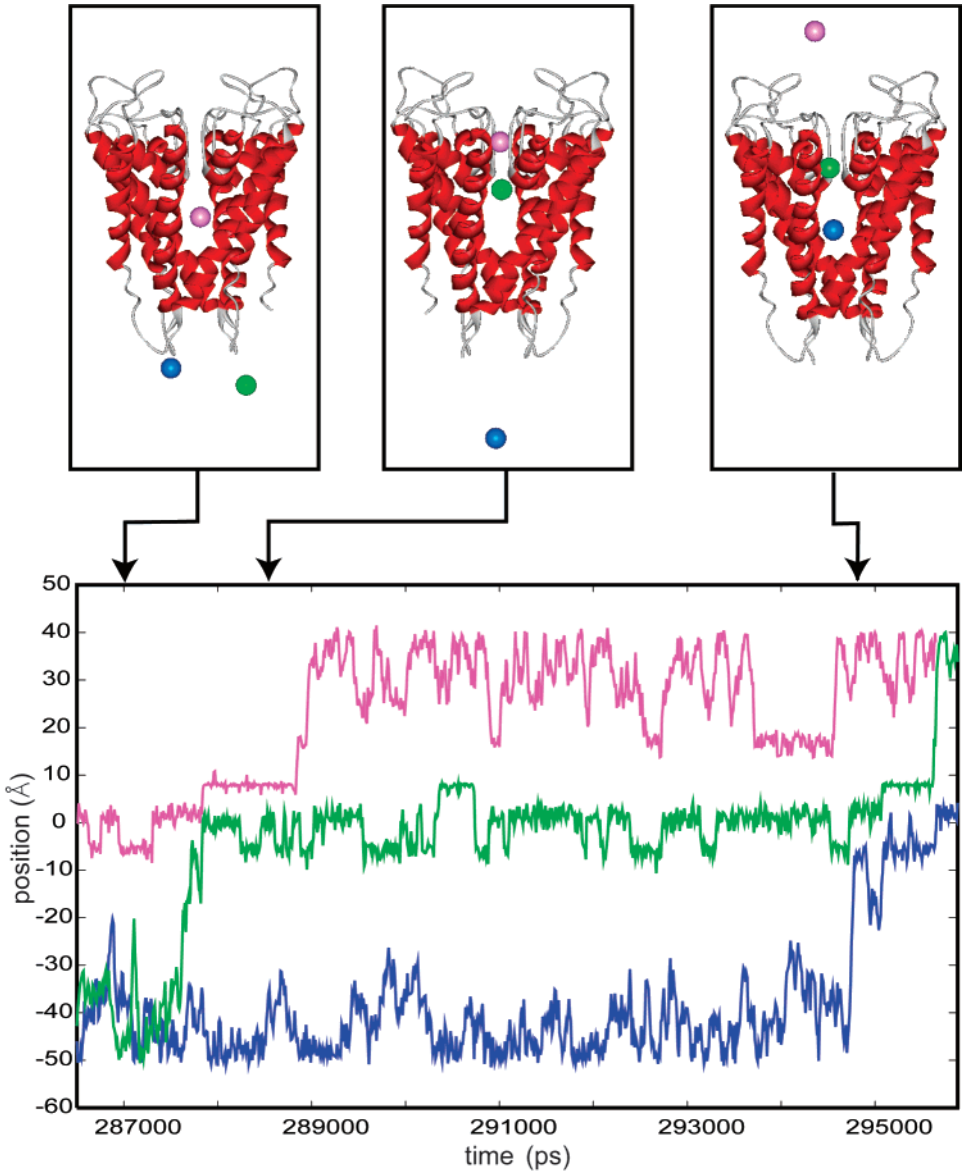

FIGURE 11. Representative result from our simulations of ion current in the KscA potassium channel. The figure presents the trajectories of some ions that are involved in the transport process (see ref 47 for details).

simulate the ion current in a realistic model of the KscA channel.[47] Typical results of our simulations are given in Figure 11. Although earlier BD simulations of KscA were reported, they did not involve sufficiently realistic electrostatic treatments (see disscusion in ref 47).

Our studies indicated that the overall time evolution is controlled by the energetics of the highest barriers. Apparently, the main role of the protein channel is to reduce the very high barrier for ion transfer through low dielectric membranes.[45,48] Nevertheless, once the barriers are calculated accurately, the evaluation of the exact time evolution requires one to use BD or related approaches.

VI. Concluding Remarks

This Account summarized our simulation studies of the dynamics of biological reactions. These studies indicated that direct MD simulations are crucial mainly for modeling of very fast reactions. Apparently, once the rate of the given process is determined by the energetics, it is possible to use "nondynamical" approaches (such as Monte Carlo methods) to determine the reaction probability.

The appeal of MD simulations is due to their ability to provide realistic descriptions of the actual molecular motions, and the ability to simulate the time evolution of reactive trajectories is very useful. Furthermore, MD simulations appear to provide a simple and effective way of averaging over protein configurations and obtaining the free energies that control biological functions. This was demonstrated in our early FEP calculations of the energetics of enzymatic reactions[49] and electrostatic free energies in proteins.[50] The field has progressed significantly since these early studies (e.g., ref 51), and much more progress is expected.

The past 25 years have taught us that we cannot predict how the field of molecular modeling will mature. Obviously, MD simulations provide a powerful tool for studies

of biological systems. It is also clear that the use of MD simulations will continue to grow with the increase of computer power. However, the use of MD simulations as a "black box" has its own risks since reproduction of an experimental observation on a complex biological system does not always increase the understanding of such a system. Dissecting the physics behind the simulated property requires more than brute-force, long-time trajectories. Here again it is important to recognize that MD simulations are not synonymous with molecular modeling and that other approaches, and in particular electrostatic calculations (e.g., refs 2 and 34), can provide the most effective way of correlating structures and functions of biological molecules. Nevertheless, there is no substitute for MD simulations in studies of fast photobiological processes.

This work was supported by NIH Grants GM24492 and GM40283. I am grateful to W. W. Parson and J. Villa for insightful discussions.

References

(1) Lifson, S.; Warshel, A. A Consistent Force Field for Calculation on Conformations, Vibrational Spectra and Enthalpies of Cycloalkanes and n-Alkane Molecules. *J. Chem. Phys.* **1968**, *49*, 5116−5129.

(2) Warshel, A.; Levitt, M. Theoretical studies of enzymic reactions: dielectric, electrostatic and steric stabilization of the carbonium ion in the reaction of lysozyme. *J. Mol. Biol.* **1999**, *103* (2), 227−249.

(3) Warshel, A. Bicycle-Pedal Model for the First Step in the Vision Process. *Nature* **1976**, *260*, 679−683.

(4) McCammon, J. A.; Gelin, B. R.; Karplus, M. Dynamics of folding proteins. *Nature* **1977**, *267*, 585−590.

(5) Warshel, A.; Parson, W. W. Dynamics of Biochemical and Biophysical Reactions: Insight from Computer Simulations. *Q. Rev. Biophys.* **2001**, *34*, 563−679.

(6) Birge, R. R. Photophysics and molecular electronic applications of the rhodopsins. *Annu. Rev. Phys. Chem.* **1990**, *41*, 683−733.

(7) Weiss, R. M.; Warshel, A. A New View of the Dynamics of Singlet cis−trans Photoisomerization. *J. Am. Chem. Soc.* **1979**, *101*, 6131−6133.

(8) Warshel, A.; Chu, Z. T. The Nature of the Surface Crossing Process in Bacteriorhodopsin: Computer Simulations of the Quantum Dynamics of the Primary Photochemical Event. *J. Phys. Chem.* **2001**, *105*, 9857−9871.

(9) Michl. Photochemical Reactions of Large Molecules. I. A Simple Physical Model of Photochemical Reactivity. *J. Mol. Photochem.* **1972**, *4*, 243, 257, 287.

(10) Warshel, A.; Barboy, N. Energy Storage and Reaction Pathways in the First Step of the Vision Process. *J. Am. Chem. Soc.* **1982**, *104*, 1469−1480.

(11) Busch, G. E.; Applebury, M. L.; Lamola, A. A.; Rentzepis, P. M. Formation and decay of prelumirhodopsin at room temperature. *Proc. Natl. Acad. Sci. U.S.A.* **1972**, *69*, 2802−2806.

(12) Mathies, R. A.; Brito Cruz, C. H.; Pollard, W. T.; Shank, C. V. Direct observation of the femtosecond excited-state cis−trans isomerization in bacteriorhodopsin. *Science* **1988**, *240*, 777−779.

(13) Henderson, R.; Baldwin, J. M.; Ceska, T. A.; Zemlin, F.; Beckman, E.; Downing, K. H. Model for the Structure of Bacteriorhodopsin Based on High-resolution Electron Cryo-microscopy. *J. Mol. Biol.* **1990**, *213*, 899−929.

(14) Warshel, A.; Chu, Z. T.; Hwang, J.-K. The Dynamics of the Primary Event in Rhodopsins Revisited. *Chem. Phys.* **1991**, *158*, 303−314.

(15) Ben-Nun, M.; Molnar, F.; Lu, H.; Philips, J. C.; Martinez, T. J.; Schulten, K. Quantum dynamics of the femtosecond photoisomerization of retinal in bacteriorhodopsin. *Faraday Discuss.* **1998**, *110*, 447−462.

(16) Warshel, A. Dynamics of Reactions in Polar Solvents. Semiclassical Trajectory Studies of Electron-Transfer and Proton-Transfer Reactions. *J. Phys. Chem.* **1982**, *86*, 2218−2224.

(17) Churg, A. K.; Warshel, A. Modeling the Activation Energy and Dynamics of Electron-Transfer Reactions in Proteins. In *Structure and Motion: Membranes, Nucleic Acids and Proteins*; Clementi, E., et al., Eds.; Adenine Press: Guilderland, NY, 1985; p 361.

(18) Creighton, S.; Hwang, J.-K.; Warshel, A.; Parson, W. W.; Norris, J. Simulating the Dynamics of the Primary Charge Separation Process in Bacterial Photosynthesis. *Biochemistry* **1988**, *27*, 774−781.

(19) Warshel, A.; Parson, W. W. Computer Simulations of Electron-Transfer Reactions in Solution and Photosynthetic Reaction Centers. *Annu. Rev. Phys. Chem.* **1991**, *42*, 279−309.

(20) Deisenhofer, J.; Epp, O.; Sinning, I.; Michel, H. Crystallographic refinement at 2.3 Å resolution and refined model of the photosynthetic reaction centre from *Rhodopseudomonas viridis*. *J. Mol. Biol.* **1995**, *246*, 429−457.

(21) Fleming, G. R.; Martin, J.-L.; Breton, J. Rates of primary electron transfer in photosynthetic reaction centers and their mechanistic implications. *Nature* **1988**, *33*, 190−192.

(22) Chang, C. H.; El-Kabbani, O.; Tiede, D.; Norris, J.; Schiffer, M. Structure of the membrane-bound protein photosynthetic reaction center from *Rhodobacter sphaeroides*. *Biochemistry* **1991**, *30*, 5352−5360.

(23) Alden, R. G.; Parson, W. W; Chu, Z. T.; Warshel, A. Calculations of Electrostatic Energies in Photosynthetic Reaction Centers. *J. Am. Chem. Soc.* **1995**, *117*, 12284−12298.

(24) Holzwarth, A. R.; Muller, M. G. Energetics and kinetics of radical pairs in reaction centers from *Rhodobacter sphaeroides*. A femtosecond transient absorption study. *Biochemistry* **1996**, *35*, 11820−11831.

(25) Treutlein, H.; Schulten, K.; Niedermeier, C.; Deisenhofer, J.; Michel, H.; DeVault, D. Electrostatic control of electron transfer in the photosynthetic reaction center of *Rhodopseudomonas viridis*. In *The Photosynthetic Bacterial Reaction Center*; Breton, J., Verméglio, A., Eds.; Plenum Press: New York, 1988; pp 369−377.

(26) Marchi, M.; Gehlen, J. N.; Chandler, D.; Newton, M. Diabatic surfaces and the pathway for primary electron transfer in a photosynthetic reaction center. *J. Am. Chem. Soc.* **1993**, *115*, 4178−4190.

(27) Warshel, A.; Hwang, J.-K. Simulation of the Dynamics of Electron-Transfer Reactions in Polar Solvents: Semiclassical Trajectories and Dispersed Polaron Approaches. *J. Chem. Phys.* **1986**, *84*, 4938−4957.

(28) Warshel, A.; Chu, Z. T.; Parson, W. W. Dispersed Polaron Simulations of Electron Transfer in Photosynthetic Reaction Centers. *Science* **1989**, *246*, 112−116.

(29) Kubo, R.; Toyozawa, Y. Application of the Method of Generating Function to Radiative and Non-Radiative Transitions of a Trapped Electron in a Crystal. *Prog. Theor. Phys.* **1955**, *13*, 160−182.

(30) Villà, J.; Warshel, A. Energetics and Dynamics of Enzymatic Reactions. *J. Phys. Chem.* **2001**, *105*, 7887−7907.

(31) Warshel, A. *Computer Modeling of Chemical Reactions in Enzymes and Solutions*; John Wiley & Sons: New York, 1991.

(32) Bennet, C. H. In *Algorithms for Chemical Computations*; Christofferson, R. E., Ed.; American Chemical Society: Washington, D.C., 1977; p 63−97.

(33) Warshel, A. Dynamics of Enzymatic Reactions. *Proc. Natl. Acad. Sci. U.S.A.* **1984**, *81*, 444−448.

(34) Warshel, A. Electrostatic Basis of Structure−Function Correlation in Proteins. *Acc. Chem. Res.* **1981**, *14*, 284−290.

(35) Neria, E.; Karplus, M. Molecular Dynamics of an Enzyme Reaction: Proton Transfer in TIM. *Chem. Phys. Lett.* **1997**, *267*, 23−30.

(36) Hwang, J.-K.; Chu, Z. T.; Yadav, A.; Warshel, A. Simulations of Quantum Mechanical Corrections for Rate Constants of Hydride-Transfer Reactions in Enzymes and Solutions. *J. Phys. Chem.* **1991**, *95*, 8445−8448.

(37) Cannon, W. R.; Singleton, S. F.; Benkovic, S. J. A perspective on biological catalysis. *Nature Struct. Biol.* **1996**, *3*, 821−833.

(38) Gillan, M. J. Quantum-Classical Crossover of the Transition Rate in the Damped Double Well. *J. Phys. C. Solid State Phys.* **1987**, *20*, 3621−3641.

(39) Voth, G. A.; Chandler, D.; Miller, W. H. Rigorous Formulation of Quantum Transition State Theory and Its Dynamical Corrections. *J. Chem. Phys.* **1989**, *91*, 7749−7760.

(40) Sham, Y.; Muegge, I.; Warshel, A. Simulating proton translocations in proteins: Probing proton-transfer pathways in the *Rhodobacter Sphaeroides* Reaction Center. **1999**, *36*, 484−500.

(41) Åqvist, J.; Warshel, A. Energetics of Ion Permeation Through Membrane Channels. Solvation of Na^+ by Gramicidin A. *Biophys. J.* **1989**, *56*, 171−182.

(42) Okamura, M. Y.; Paddock, M. L.; Graige, M. S.; Feher, G. Proton and electron transfer in bacterial reaction centers. *Biochim. Biophys. Acta* **2000**, *1458*, 148−163.

(43) Warshel, A. Conversion of Light Energy to Electrostatic Energy in the Proton Pump of *Halobacterium halobium*. *Photochem. Photobiol.* **1979**, *30*, 285−290.

(44) Doyle, D. A.; Cabral, J. M.; Pfuetzner, R. A.; Kuo, A. L.; Gulbis, J. M.; Cohen, S. L.; Chait, B. T.; MacKinnon, R. The structure of the potassium channel: Molecular basis of K^+ conduction and selectivity. *Science* **1998**, *280*, 69−77.
(45) Åqvist, J.; Luzhkov, V. Ion permeation mechanism of the potassium channel. *Nature* **2000**, *404*, 881−884.
(46) Ranatunga, K. M.; Shrivastava, I. H.; Smith, G. R.; Sansom, M. S. P. Side-chain ionization states in a potassium channel. *Biophys. J.* **2001**, *80*, 1210−1219.
(47) Burykin, A.; Schutz, C. N.; Villà, J.; Warshel, A. Simulations of Ion Current in Realistic Models of Ion Channels: The KcsA Potassium Channel. *Proteins: Struct., Func., Genet.*, in press.
(48) Warshel, A.; Russell, S. T. Calculations of Electrostatic Interactions in Biological Systems and in Solutions. *Q. Rev. Biophys.* **1984**, *17*, 283−421.
(49) Warshel, A. Simulating the Energetics and Dynamics of Enzymatic Reactions. Specificity in Biological Interactions. *Pontif. Acad. Sci. Scr. Varia* **1984**, *55*, 60−81.
(50) Warshel, A.; Sussman, F.; King, G. Free Energy of Charges in Solvated Proteins: Microscopic Calculations Using a Reversible Charging Process. *Biochemistry* **1986**, *25*, 8368−8372.
(51) Kollman, P. Free Energy Calculations: Applications to Chemical and Biochemical Phenomena. *Chem. Rev.* **1993**, *93*, 2395−2417.

AR010033Z